The Astronomical Journal, 148:48 (8pp), 2014 September doi:10.1088/0004-6256/148/3/48

SEPARATED FRINGE PACKET OBSERVATIONS WITH THE CHARA ARRAY. II. ω ANDROMEDA, HD 178911, AND ξ CEPHEI

C. D. Farrington[1], T. A. ten Brummelaar[1], B. D. Mason[2], W. I. Hartkopf[2], D. Mourard[3], E. Moravveji[4], H. A. McAlister[5], N. H. Turner[1], L. Sturmann[1], and J. Sturmann[1]
[1] The CHARA Array, Mount Wilson Observatory, Mount Wilson, CA 91023, USA; farrington@chara-array.org, theo@chara-array.org, nils@chara-array.org, sturmann@chara-array.org, judit@chara-array.org
[2] US Naval Observatory, 3450 Massachusetts Avenue NW, Washington, DC 20392-5420, USA; bdm@usno.navy.mil, wih@usno.navy.mil
[3] Université de Nice Sophia Antipolis, CNRS, Laboratoire J. L. Lagrange, Observatoire de la Côte d'Azur—BP4209, F-06304 Nice Cedex, France; denis.mourard@oca.eu
[4] Instituut Voor Sterrenkunde, KU Leuven, Celestijnenlaan 200D, B-3001 Leuven, Belgium; Ehsan.Moravveji@ster.kuleuven.be
[5] Center for High Angular Resolution Astronomy, Georgia State University, P.O. Box 3969, Atlanta, GA 30302-3969, USA; hal@chara.gsu.edu
Received 2013 December 23; accepted 2014 June 9; published 2014 July 31

ABSTRACT

When observed with optical long-baseline interferometers, components of a binary star that are sufficiently separated produce their own interferometric fringe packets; these are referred to as separated fringe packet (SFP) binaries. These SFP binaries can overlap in angular separation with the regime of systems resolvable by speckle interferometry at single, large-aperture telescopes and can provide additional measurements for preliminary orbits lacking good phase coverage, help constrain elements of already established orbits, and locate new binaries in the undersampled regime between the bounds of spectroscopic surveys and speckle interferometry. In this process, a visibility calibration star is not needed, and the SFPs can provide an accurate vector separation. In this paper, we apply the SFP approach to ω Andromeda, HD 178911, and ξ Cephei with the CLIMB three-beam combiner at the CHARA Array. For these systems we determine component masses and parallax of $0.963 \pm 0.049\,M_{\odot}$ and $0.860 \pm 0.051\,M_{\odot}$ and 39.54 ± 1.85 mas for ω Andromeda, for HD 178911 of $0.802 \pm 0.055\,M_{\odot}$ and $0.622 \pm 0.053\,M_{\odot}$ with 28.26 ± 1.70 mas, and masses of $1.045 \pm 0.031\,M_{\odot}$ and $0.408 \pm 0.066\,M_{\odot}$ and 38.10 ± 2.81 mas for ξ Cephei.

Key words: binaries: close – binaries: spectroscopic – infrared: stars – stars: individual (ω Andromeda, HD 178911, ξ Cephei) – techniques: high angular resolution – techniques: interferometric

Online-only material: color figures, machine-readable and VO table

1. INTRODUCTION

Long-baseline interferometric telescope arrays are well-suited for observing binaries with angular separations in the sub-millarcsecond regime using the traditional interferometric visibility method (for examples, see Armstrong et al. 1992; Boden et al. 1999; Hummel et al. 1995; and Raghavan et al. 2009). Another approach (Dyck et al. 1995; Lane & Muterspaugh 2004; Bagnuolo et al. 2006; ten Brummelaar et al. 2011) applies to stellar systems where the components of a binary are sufficiently far apart in projected angular separation that their fringe packets do not overlap and the visibility fitting approach is not relevant. This paper follows Farrington et al. (2010; hereafter referred to as Paper I) presenting the results from a program of separated fringe packet (SFP) observations of spectroscopic and visual binary star systems made with the CHARA Array at Mount Wilson Observatory (ten Brummelaar et al. 2005). Paper I contained the systems χ Draconis, HD 184467, and HD 198084, and presented new observations, orbits, and masses for each system, and a variant of this technique is presented for triple systems in O'Brien et al. (2011). As part of this ongoing effort, we present here 150 new vector measurements of ω Andromeda, HD 178911, and ξ Cephei that are combined into 60 positional observations of the components of these systems. With this second paper, we have refined the process of data collection and reduction to incorporate the increased capacity and efficiency of the CLIMB (CLassic Interferometry with Multiple Baselines) beam combiner (ten Brummelaar et al. 2013).

2. OBSERVATIONAL OVERVIEW

Data were routinely taken on the CHARA Array's three largest baselines (S1–E1–W1) and other intermediate baselines when the preferred telescopes were assigned to other simultaneous observing experiments. A list of observations for ω Andromeda, HD 178911, and ξ Cephei taken with the CHARA Array, along with baselines used, is given in Table 1. This table contains the acquired one-dimensional (1D) measurements in Columns 3–6 and the two-dimensional (2D) positional calculation obtained from the observations in Columns 7–9. Each 1D measurement consists of averaged time, length of baseline, and position angle of the projected baseline at the midpoint of the 5 minute recording sequence and a separation between the peaks of the two average fringe envelopes that have been summed over the course of the data file (see Farrington et al. 2010). The 2D columns represent the combination of all the 1D data for a given set of observations through the program described in the Data Reduction section below. The exceptions to the above descriptions are those data labeled "VEGA" in the table. These measurements do not use the SFP method but visibility modulation typical for interferometers, and thus do not consist of 1D vector measurements. Full details of the VEGA instrument can be found in Mourard et al. (2009).

Before 2009, observations for the SFP program were taken as described in Paper I with the CHARA Classic two-beam combiner as described by ten Brummelaar et al. (2005). All observations after 2009 were taken with the CHARA CLIMB IR pupil-plane three-beam combiner (ten Brummelaar et al. 2013)

Table 1
CHARA SFP Observations

System	Set	MJD	B (m)	θ (°)	ρ (mas)	BY	θ	ρ (mas)
ω And	1	54786.29163	329.24	9.76	9.58			
		54786.29637	329.34	8.66	12.03			
		54786.38633	329.91	347.51	22.61			
		54786.39170	328.73	346.32	22.76	2008.8772	117.03	35.24
	2	55105.79028	VEGA			2009.7500	232.57	24.68
	3	55111.30572	321.05	30.97	23.42			
		55111.35179	326.94	20.93	21.19			
		55111.36393	274.44	136.19	9.62			
		55111.42817	303.61	51.56	27.38	2009.7670	245.23	28.61
	4	55115.27366	278.40	335.77	$\lesssim$5			
		55115.28937	320.12	31.97	25.14			
		55115.32751	325.76	23.82	20.66			
		55115.37560	311.93	63.05	29.19			
		55115.42699	300.57	43.31	26.79			
		55115.43530	250.00	119.11	18.47	2009.7780	246.85	29.20
	5	55154.73407	VEGA			2009.8844	273.55	38.67

Notes. Observation log for ω Andromeda, HD 178911, and ξ Cephei on the CHARA Array from 2005 to 2012. Each set of vector observations (along with the projected baseline length and epoch of observation) in Columns 3–6 were combined to create the true location of the secondary and average time of all the data points defined in the last three columns. Errors for all measurements in the final column are ≈1 mas.

(This table is available in its entirety in machine-readable and Virtual Observatory (VO) forms in the online journal. A portion is shown here for guidance regarding its form and content.)

also through the K' filter. The time span between observing sessions ranged from as little as a week to more than a year. Orbits for these systems were determined with combined spectroscopic/interferometric solutions as described in Tokovinin (1992, 1993) with all available CHARA, published speckle interferometry data (Hartkopf et al. 2001b), and spectroscopic orbits as described below.

2.1. Characterizing Separated Fringe Packets

The theory, history, errors, and method of utilizing SFP interferometry are discussed in detail in Paper I. Several important changes have been implemented since the publication of that paper that have increased the accuracy, quality, and speed of the data acquisition with the CHARA Array. In 2009, the new CLIMB three-beam combiner (Sturmann et al. 2010) was built alongside of the previously used CLASSIC two-beam combiner. While primarily built for multiple simultaneous baseline observations to determine closure phase (ten Brummelaar et al. 2012), the SFP project found an alternative use for the combiner, as the primary mode for CLIMB used two dither mirrors working simultaneously at different frequencies and movement parameters narrowed the delay-space being sampled at any given time. If used in its primary mode, this would decrease the 1D sky coverage of two of the baselines by 25% for the second pair of baselines that include a dither mirror, and 50% for the final pair which is considered the "cross fringe." In order to retain the largest possible sky coverage, a two-beam mode was added that used the same frequencies and largest possible delay-space search for all three baselines, but only recorded one baseline at a time. With this mode on CLIMB, the amount of time needed to observe one object on all three baselines took less than a quarter of the time required by the method described in Paper I.

2.2. Data Reduction

Most of the data reduction was done with the same method and software as described in Farrington et al. (2010) with the exception of the final stage, the determination of the 2D location of the companion.

2.2.1. Calculation Method for Astrometry from SFP Data

Each observation of a binary star produces a linear separation of the system on the sky, whose direction is determined by the projection angle of the baseline on the sky and whose distance is determined by the separation of the two fringe packets divided by the projected baseline length (Farrington et al. 2010). Thus, if we place the primary, as defined by the star that produces the largest fringe packet,[6] at the origin, each observation will produce a line, which for observation i we write as

$$y = m_i x + c_i. \quad (1)$$

For any single observation, the position of the secondary (x_s, y_s) can lie anywhere on this line, but for more than one observation the position of the secondary is more restricted. Ideally all of the lines will intersect at the position of the secondary, but of course the presence of noise makes this extremely unlikely. We therefore use the equivalent of a χ^2 minimization.

We write the distance of the secondary from the line defined by observation i as

$$\Delta_i = \sqrt{(x_s - x_p)^2 + (y_s - y_p)^2}, \quad (2)$$

[6] Note that the star that produces the largest fringe packet is not necessarily the brightest star as the brightest star may be more resolved at the current baseline than the fainter star and its fringe packet is suppressed.

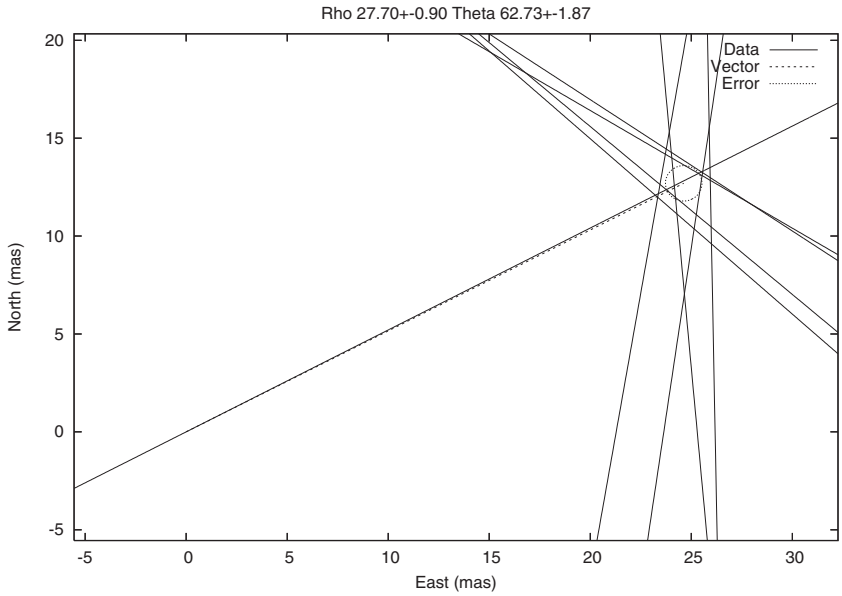

Figure 1. Example vector separation plot for ω Andromeda, 2012.5615. An example output from the SFPAstrom program that solves for the location of the companion from multiple 1D vector measurements. The dashed line is the vector from the origin to the estimated location of the companion. Each solid line is one 1D vector measurement, and the dashed circle is the error ellipse for the best estimate for the position of the secondary and the size of the ellipse represents the error of the secondary position.

where (x_p, y_p) is the point on the line defining the perpendicular distance between (x_s, y_s) and the line given by

$$x_p = \frac{x_s + m_i y_s - m_i c_i}{1 + m_i^2} \tag{3}$$

and

$$y_p = m_i x_p + c_i. \tag{4}$$

We then say that the χ^2 of any secondary position is given by

$$\chi^2 = \sum_{i=1}^{N_{obs}} \frac{\Delta_i^2}{\sigma_i^2}, \tag{5}$$

where σ_i^2 is the variance of the linear separation of observation i. Following standard χ^2 analysis, we say that the best estimate for the position of the secondary is given by the values of (x_s, y_s) that minimize χ^2. Since this is not a true χ^2 measurement, the error cannot be estimated in the normal way. Instead we use the standard deviation of the perpendicular distances, Δ_i. A program was written in C by T. A. ten Brummelaar that does the above calculations called "SFPAstrom" and a sample output of the resulting fits is displayed in Figure 1.

2.3. Effects of Misalignment

In Paper I, the most prevalent possible sources of error were discussed and all but the piston error were of such a small magnitude that they could essentially be dismissed. It is worth quantifying the potential error in separation of two fringe packets brought about by the misalignment of the optical path from the beam combiner out to the telescope on one arm of the interferometer.

Starting with the configuration in Figure 2, we can calculate the error in the path of a single star for a typical misalignment that could occur due to coudé variation in azimuth of approximately 5 mm or about 10″ over the longest baseline. We want to determine χ_1 and χ_2 in terms of the nominal distances (d_1 and d_2), the angle of the telescope, θ, and the misalignment angle, α. From simple geometric identities, it can be shown that

$$\chi_1 = \frac{d_1 \sin\left(\frac{\alpha}{2} - \frac{\theta}{2}\right)}{\sin\left(\frac{3\alpha}{2} - \frac{\theta}{2}\right)} \tag{6}$$

and

$$\chi_2 = \frac{d_2 \sin\left(\frac{3\alpha}{2} + \frac{\theta}{2}\right)}{\sin\left(\frac{\alpha}{2} + \frac{\theta}{2}\right)}. \tag{7}$$

For the pertinent case where we are observing a binary system that would produce two fringes as described in Paper I, we show that the path difference for the individual components for a relatively wide realistic case

$$\chi_1(\theta) + \chi_2(\theta) - \chi_1(\theta + \Delta) - \chi_2(\theta + \Delta) \ll \boldsymbol{\rho}_{\mu m}, \tag{8}$$

where Δ is the on-sky separation of the two fringes in milliarcseconds and rearranging Equation (5) from Paper I gives

$$\boldsymbol{\rho}_{\mu m} = \frac{\boldsymbol{\rho}_{mas} B(m)}{206.265}. \tag{9}$$

The solutions for Equation (8) are given in Figure 3 with increasing θ and, from 0″–10″ misalignment for a baseline of 300 m and projected binary star separation of 60 mas, show a maximum differential delay that is three orders of magnitude smaller than the separation between the two fringes (for this example, the separation of the fringes in microns is approximately 87 μm, and the error due to the largest misalignment approaches 0.08 μm), and thus far smaller than the atmospheric piston, the most dominant source of positional error.

3. RESULTS

3.1. ω Andromeda

ω Andromeda = HR 417, HD 8799, spectral types are suggested to be F3V+F5V (Abt 1985; Cowley 1976). The listed

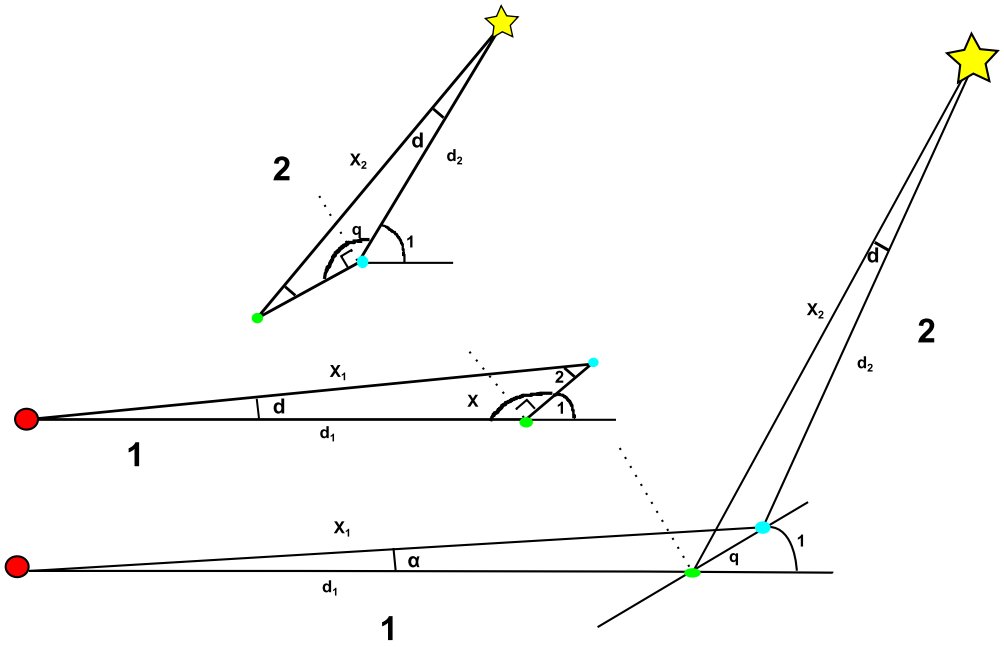

Figure 2. Simple diagram of the components comprising beam path from the beam combiner to the observed system. The distances χ_1 and χ_2 are the misaligned paths when d_1 and d_2 are the optical axis when the alignment is done correctly, α is the angle subtended by the path difference between the beam combiner and the telescope, and θ is the angle of the telescope with 0 at zenith and 90 at the horizon. The difference between the χ and d paths is calculated in terms of α and θ.
(A color version of this figure is available in the online journal.)

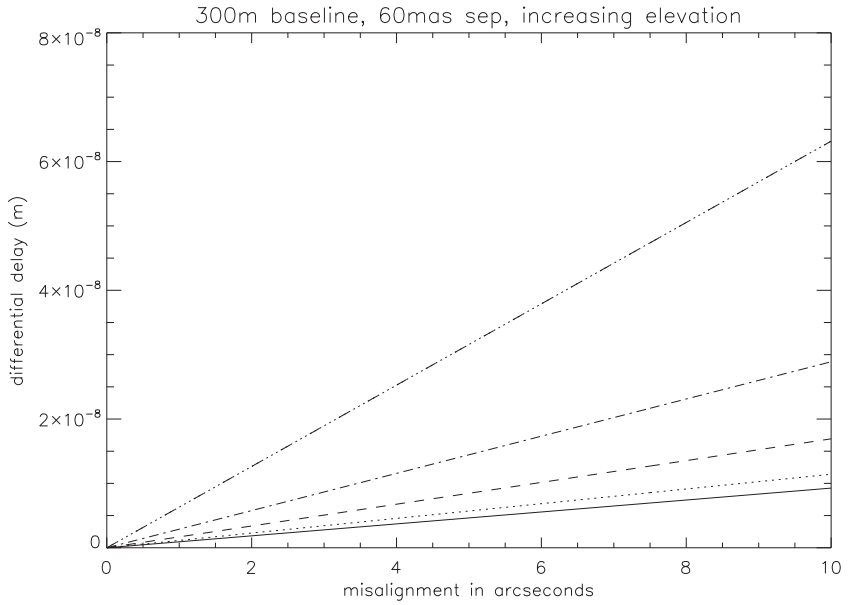

Figure 3. Calculated differential delay based on telescope angle and realistic beam misalignment. The lines correspond to angles from near the horizon to near zenith (solid line near zenith, each line after decreases the zenith angle by 15°, ending at 30° above the horizon) and represent the difference between the single and double star cases described in Equation (8) compared to the ideal path case of approximately 1 μm.

B component is faint (12th magnitude at 2″) and may be optical (Burnham 1873, 1887). The system also contains a second pair 2′ distant, separated by 5″ with a combined magnitude of 10, designated as components CD, which are optical. No previous astrometric or interferometric observations of the system have been published. All astrometric data taken for this system was obtained on the CHARA Array using CLIMB and the VEGA visible beam combiner (Mourard et al. 2009). VEGA data are not processed through the SFP principle but they used the classical principle of visibility modulation as a function of time, baseline, as in Pan et al. (1990). The spectroscopic orbit used in the combined solution presented here is from Griffin (2011). A simultaneous solution utilizing all the radial velocity and visual data was carried out with an interactive program developed by Tokovinin (1992, 1993) that computes all 10 orbital elements. This technique employs the method of least squares to yield elements satisfying both radial velocity and astrometric measurements as described in McAlister et al. (1995). The orbital elements from the combined solution are listed in Table 2, along with the orbital χ^2_ν, masses, and orbital parallax calculated from the solution, and Figure 4 shows the relative orbit. The orbital parallax of 39.54 ± 1.85 mas

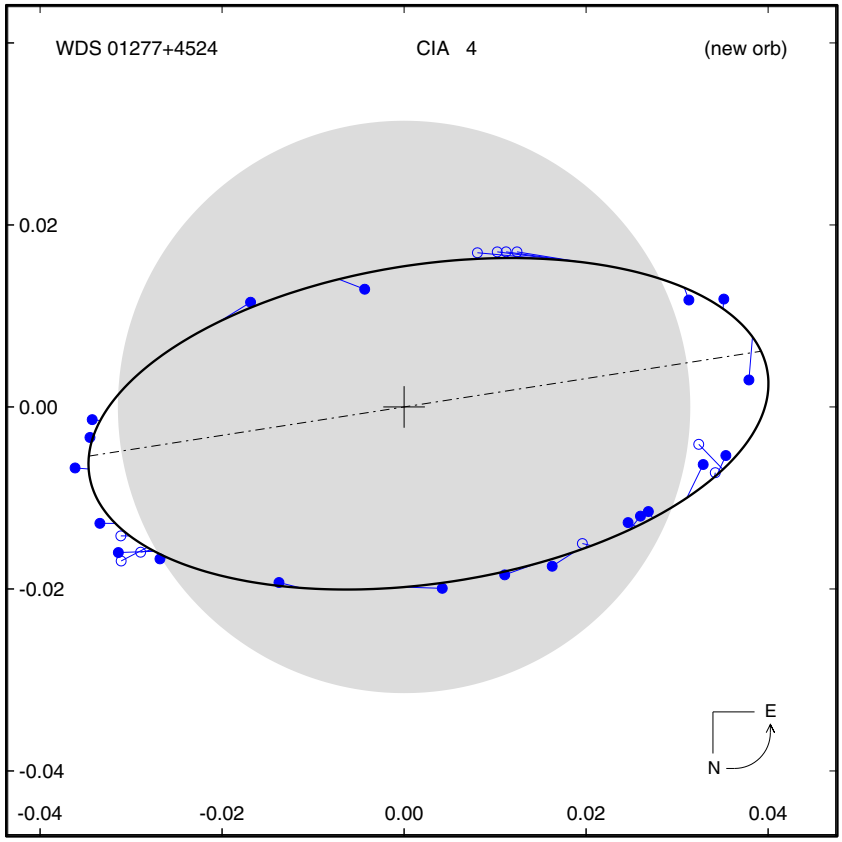

Figure 4. Orbit plot for ω Andromeda. Combined visual-spectroscopic solution from this paper (solid line) using all available data which is all from the CHARA Array SFP program. The shaded circle represents the resolution limit of a speckle interferometry camera on a 4 m telescope and is shown to aid in scaling. The dot–dashed line indicates the line of nodes. The VEGA beam combiner measures are shown as open circles. The CHARA Array SFP measures are indicated with filled circles. All measurements are connected to their predicted positions on the orbit by "$O-C$" lines. The direction of motion is indicated on the northeast orientation in the lower right of the plot. The scales at left and bottom are in arcseconds.

(A color version of this figure is available in the online journal.)

Table 2
ω Andromeda Orbital Elements and Calculated Values

Elements	This Paper
P (days)	254.9003 ± 0.1960
(yr)	0.69789 ± 0.00054
T_0 (MJD)	54214.835 ± 3.187
(BY)	2007.3110 ± 0.0087
a ($''$)	0.038 ± 0.001
e	0.142 ± 0.012
i ($^\circ$)	62.49 ± 2.10
ω ($^\circ$)	278.87 ± 2.01
Ω ($^\circ$)	115.94 ± 4.38
K_1 (km s^{-1})	17.54 ± 0.30
K_2 (km s^{-1})	19.62 ± 0.30
γ_0 (km s^{-1})	14.83 ± 0.17
χ^2_ν (RV)	106.53
χ^2_ν (VIS)	15.59
χ^2_ν (Combined)	84.29
M_P ($M_\odot$)	0.993 ± 0.056
M_S ($M_\odot$)	0.888 ± 0.058
π_{orb} ($''$)	0.03912 ± 0.00197
π_{Hip} ($''$)	0.03494 ± 0.0031

is different from that of *Hipparcos* (34.94 ± 0.31 mas; van Leeuwen 2007), probably due to the pair being unresolved and the parallax being biased with the binary separation. The calculated masses are $0.963 \pm 0.049\ M_\odot$ and $0.860 \pm 0.051\ M_\odot$ for the components and an orbital grade of 1 determined by criteria of the Sixth Orbital Catalog (Hartkopf et al. 2001a).

3.2. HD 178911

HD 178911 = HR 7272, CHR 84Aa, Ab, spectral types are G1V+K1V. Measured diameter is 0.114 mas (Ribas et al. 2003). The AB pair ($16''$, $\Delta m = 1.1$) is known as STF2747 and shares a common proper motion. The B component of the wide pair is an extra solar planet host star (Wittenmyer et al. 2009). The much wider AC pair is known as WAL 105 ($96''$, $\Delta m = 4.6$) and is optical. The close Aa, Ab pair was discovered by the CHARA speckle interferometry program in 1985 (McAlister et al. 1987). Summary information for components can be found in the Washington Double Star (WDS) Catalog (Mason et al. 2001). The entry from the Sixth Visual Orbit Catalog (ORB6; Hartkopf et al. 2001a) is from Hartkopf et al. (2000), and the spectroscopic orbit and first combined solution are from Tokovinin et al. (2000). While the previous orbit included only six visual measurements, our solution is quite similar with reduced errors while including 17 measurements from the CHARA Array, and 10 other subsequent speckle interferometric data points. This five-fold increase in the number of measures of relative astrometry has a significant impact on the mass and other determinations due to much lower errors. The orbit, presented in Table 3, was computed using the same combined solution technique of Tokovinin (1992, 1993) listed above deriving all 10 orbital parameters as well as orbital χ^2_ν, component masses,

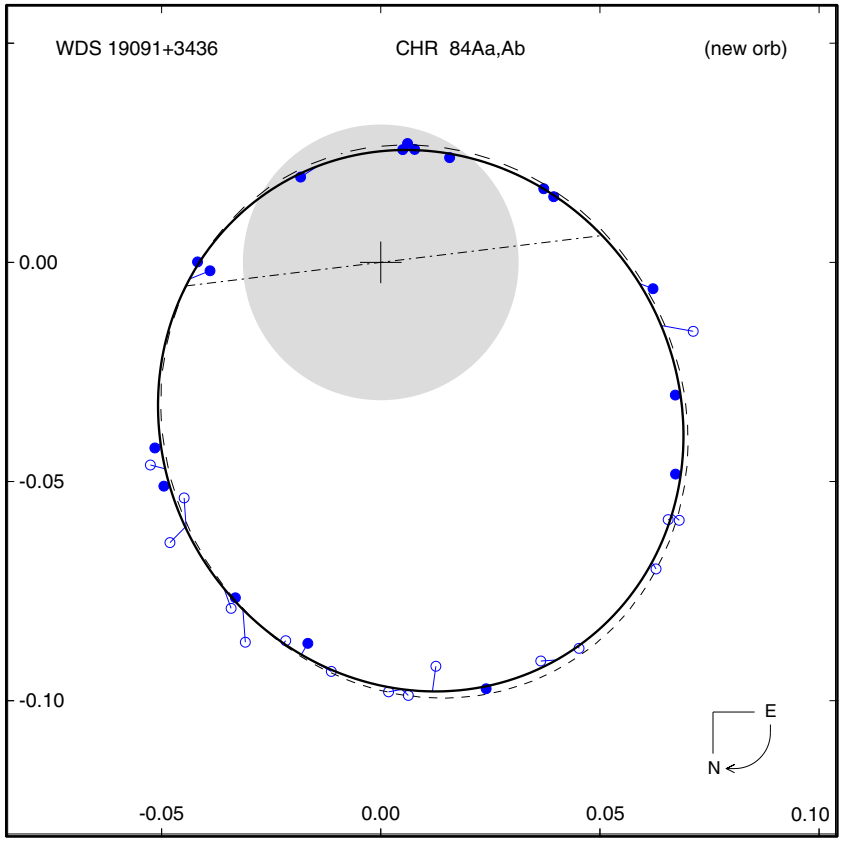

Figure 5. Orbit plot for HD 178911. Combined visual-spectroscopic solution from this paper (solid line) using all available data which is consistent with the previous orbit of Tokovinin et al. (2000; dashed line). The shaded circle represents the resolution limit of a speckle interferometry camera on a 4 m telescope. The CHARA Array SFP measures are indicated with filled circles. Speckle interferometry measurements are indicated as open circles. Other symbols as Figure 4.

(A color version of this figure is available in the online journal.)

Table 3
HD 178911 Orbital Elements and Calculated Values

Elements	Tokovinin et al. (2000)	This Paper
P (days)	1296.3 ± 1.1	1296.984 ± 0.355
(yr)	3.55 ± 0.003	3.55102 ± 0.00097
T_0 (MJD)	50572.2 ± 1.5	50574.953 ± 1.302
(BY)	1997.337 ± 0.00411	1997.34538 ± 0.00356
a ($''$)	0.0735 ± 0.0026	0.074 ± 0.002
e	0.589 ± 0.004	0.597 ± 0.003
i (°)	150.1 ± 3.7	147.29 ± 0.99
ω (°)	262.5 ± 0.8	83.88 ± 0.87
Ω (°)	276.7 ± 1.5	276.91 ± 1.45
K_1 (km s^{-1})	6.57 ± 0.04	6.47 ± 0.09
K_2 (km s^{-1})	8.53 ± 0.17	8.33 ± 0.18
γ_0 (km s^{-1})	−41.01 ± 0.03	−41.04 ± 0.06
χ^2_ν (RV)		0.685
χ^2_ν (VIS)		2.187
χ^2_ν (Combined)		0.997
M_P ($M_\odot$)	1.07 ± 0.37	0.802 ± 0.055
M_S ($M_\odot$)	0.84 ± 0.29	0.622 ± 0.053
π_{orb} ($''$)	0.025 ± 0.008	0.02826 ± 0.00170

and orbital parallax. Figure 5 plots the previous and current orbital solutions with all measurements previous to this effort. The orbital parallax of 28.26 ± 1.70 mas is different from that of *Hipparcos* (19.11 ± 2.35 mas; van Leeuwen 2007), probably due to the pair being unresolved and the parallax being affected by the binary separation. Using the objective orbit grading scheme described in ORB6 a grade of 1, definitive, has been determined for this pair. As with all other orbits in ORB6, this is based only on the orbital elements and the resolved measures and, therefore, does not take into account the spectroscopic solution which significantly improves the quality. The calculated masses of 0.802 ± 0.055 $M_\odot$ and 0.622 ± 0.053 $M_\odot$ for the Aa and Ab components, while lower, are within the error margin of the previous solution.

3.3. ξ *Cephei A*

ξ Cephei A = HR 8417, HD 209790, MCA 69Aa, Ab. The AB (5″–8″, $\Delta m = 2.0$) and AC (110″, $\Delta m = 8.2$) pairs are both known as STF2863. B shares a common proper motion with A. The C component has only been measured a few times since its discovery in 1925 (Öpik 1932) and its status, whether optical or physical, is unknown. Eggen (1991, 1992) has determined the system to be a member of the IC 2391 supercluster. Summary information for the system can be found in the WDS Catalog (Mason et al. 2001). Hyneck (1938) included the close pair in a list of composite spectrum binaries, and Abt (1961) suggested that it is a long-period spectroscopic binary. Vickers & Scarfe (1976) confirmed Abt's suspicion, finding the system to be double-lined with an orbital period of 811 days. From an analysis of colors, Vickers & Scarfe assigned spectral types of A7 for Aa and F5 for Ab, suspecting on the basis of strong lines of strontium and ionized iron that the secondary is a subgiant. The fit to the colors leads to a $\Delta V = 0.3$ mag, a value significantly smaller than that expected for a pair of A7 and F5 dwarfs, lending further support to the evolved nature of the secondary. Vickers

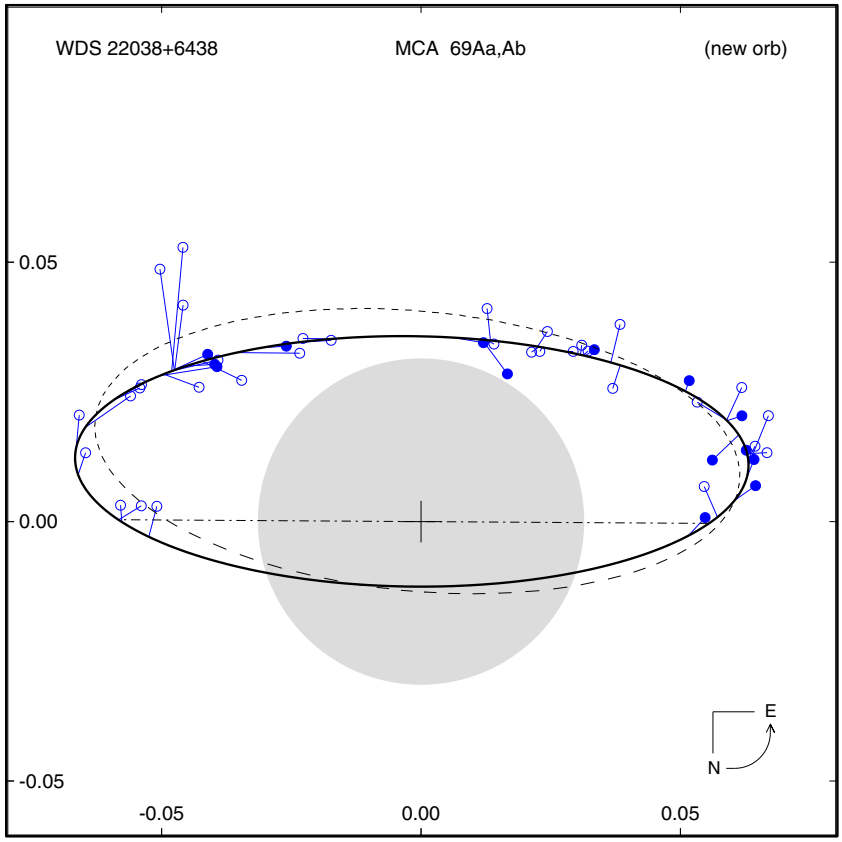

Figure 6. Orbit plot for ξ Cephei. The figure shows the relative visual orbit of the system; the x and y scales are in arcseconds. The solid curve represents the orbit determined in this paper with the dashed curve denoting the orbit of Pourbaix (2000). Other symbols as Figure 5.

(A color version of this figure is available in the online journal.)

& Scarfe also measured the radial velocity of the B component and found it indistinguishable from the γ-velocity of the Aa, Ab system, confirming the common proper motion physicality. The system Aa, Ab was subsequently resolved by speckle interferometry (McAlister 1977) and in McAlister (1980) the first relative orbit was derived from 10 speckle observations and compared with the spectroscopic orbit of Vickers & Scarfe (1976).

The passage of time has quadrupled the number of interferometric measurements, most recently in the SFP campaign with the CHARA Array, and more importantly, this has increased the phase coverage from 1.3 to 16.4 orbital revolutions. All published observations of the pair are listed in the Fourth Interferometric Catalog (Hartkopf et al. 2001b) including the recent measures by speckle interferometry by Horch et al. (2008, 2010). The orbit, as presented in Table 4, was computed using the same combined solution technique of Tokovinin (1992, 1993) listed above and plotted in Figure 6. As above, the orbital parallax of 38.10 ± 2.81 mas is different from that of *Hipparcos* (33.79 ± 1.06 mas; van Leeuwen 2007), probably due to the pair being unresolved and the parallax again being biased by the binary separation. Using the objective orbit grading scheme described in ORB6, a grade of 2, good, has been determined for this pair. As above this is based only on the orbital elements and the resolved measures and does not take into account the spectroscopic solution which significantly improves the quality. The masses of $1.045 \pm 0.031\ M_{\odot}$ and $0.408 \pm 0.066\ M_{\odot}$ for the components are of the same order as the previous solutions but are significantly different from what should be expected from a system with spectral types listed above.

Table 4
ξ Cephei Orbital Elements and Calculated Values

Elements	Pourbaix (2000)	This Paper
P (days)	818.51 ± 0.98	819.9402 ± 0.6082
(yr)	2.241 ± 0.0027	2.24492 ± 0.00167
T_0 (MJD)	40949.584 ± 3.36	40949.144 ± 3.973
(BY)	1970.992 ± 0.0092	1970.9908 ± 0.0105
a ($''$)	0.072 ± 0.0017	0.074 ± 0.004
e	0.50 ± 0.021	0.481 ± 0.024
i ($^\circ$)	68 ± 1.4	70.96 ± 1.72
ω ($^\circ$)	273 ± 1.1	272.98 ± 1.95
Ω ($^\circ$)	85 ± 1.9	89.64 ± 3.51
K_1 (km s^{-1})	7.16 ± 0.56	7.81 ± 0.50
K_2 (km s^{-1})	19.82 ± 0.55	19.98 ± 0.83
γ_0 (km s^{-1})	-10.74 ± 0.34	-10.59 ± 0.33
χ^2_ν (RV)		204.65
χ^2_ν (VIS)		45.01
χ^2_ν (Combined)		150.55
$M_{\rm P}$ ($M_{\odot}$)	1.00 ± 0.13	1.045 ± 0.032
$M_{\rm S}$ ($M_{\odot}$)	0.36 ± 0.05	0.409 ± 0.066
$\pi_{\rm orb}$ ($''$)	0.038 ± 0.0021	0.03811 ± 0.00282

4. CONCLUSION

As it was suggested in the first paper of this series, the inclusion of the CLIMB beam combiner did significantly increase the accuracy and alacrity of data acquisition for the SFP binary program. The three systems observed in this paper are just the first of many that are available to this technique

and the ongoing effort continues to add new spectroscopic binaries that are within the available observation range for orbit determination. It should be noted that for the three systems discussed herein, and χ Draconis from Paper I of this series, the combined orbital solutions provide masses that do not mesh well with the predicted masses assigned from spectral typing. We present these orbits as they are computed, without prejudice to previously quoted spectral types, as the spectral typing and luminosity class determination are beyond the scope of the current investigation. Additionally, five of the six objects from both this discussion and Paper I show significant differences between the orbital parallax calculated here and the *Hipparcos* parallax measurements due to the binarity unresolved at that time.

The CHARA Array, operated by Georgia State University, was built with funding provided by the National Science Foundation, Georgia State University, the W. M. Keck Foundation, and the David and Lucile Packard Foundation. This research is supported by the National Science Foundation under grant AST 0908253 and AST 1211129 as well as by funding from the office of the Dean of the College of Arts and Science at Georgia State University. This research has made use of the SIMBAD database, operated at CDS, Strasbourg, France. Thanks are also extended to the U.S. Naval Observatory for their continued support of the Double Star Program. We very much appreciate the hard work of Isabelle Tallon-Bosc for the support for this project. This research has made use of the Jean-Marie Mariotti Center `LITpro` service co-developed by CRAL, LAOG, and FIZEAU (Tallon-Bosc et al. 2008).[7]

REFERENCES

Abt, H. 1961, ApJS, 6, 37
Abt, H. 1985, ApJS, 59, 95
Armstrong, J. T., Mozurkewich, D., Vivekanand, M., et al. 1992, AJ, 104, 241
Bagnuolo, W. G., Jr., Taylor, S. F., McAlister, H. A., et al. 2006, AJ, 131, 2695
Boden, A. F., Lane, B. F., Creech-Eakman, M. J., et al. 1999, ApJ, 527, 360
Burnham, S. W. 1873, MNRAS, 33, 437
Burnham, S. W. 1887, PLicO, 1, 45
Cowley, A. P. 1976, PASP, 88, 95
Dyck, H. M., Benson, J. A., & Schloerb, F. P. 1995, AJ, 110, 1433
Eggen, O. J. 1991, AJ, 102, 2028
Eggen, O. J. 1992, AJ, 104, 2141
Farrington, C. D., ten Brummelaar, T. A., Mason, B. D., et al. 2010, AJ, 139, 2308
Griffin, R. F. 2011, Obs, 131, 225
Hartkopf, W. I., Mason, B. D., McAlister, H. A., et al. 2000, AJ, 119, 3084
Hartkopf, W. I., Mason, B. D., & Worley, C. E. 2001a, AJ, 122, 3472 (http://ad.usno.navy.mil/wds/orb6.html)
Hartkopf, W. I., McAlister, H. A., & Mason, B. D. 2001b, AJ, 122, 3480 (http://ad.usno.navy.mil/wds/int4.html)
Horch, E. P., Falta, D., Anderson, L. M., et al. 2010, AJ, 139, 205
Horch, E. P., van Altena, W. F., Cyr, W. M., et al. 2008, AJ, 136, 312
Hummel, C. A., Armstrong, J. T., Buscher, D. F., et al. 1995, AJ, 110, 376
Hynek, J. A. 1938, CoPer, 1, 10
Lane, B. F., & Muterspaugh, M. W. 2004, ApJ, 601, 1129
Mason, B. D., Wycoff, G. L., Hartkopf, W. I., Douglass, G. G., & Worley, C. E. 2001, AJ, 122, 3466
McAlister, H. A. 1977, ApJ, 215, 159
McAlister, H. A. 1980, ApJ, 236, 522
McAlister, H. A., Hartkopf, W. I., Hutter, D. J., Shara, M. M., & Franz, O. G. 1987, AJ, 93, 183
McAlister, H. A., Hartkopf, W. I., Mason, B. D., et al. 1995, AJ, 110, 366
Mourard, D., Clausse, J. M, Marcotto, A., et al. 2009, A&A, 508, 1073
O'Brien, D. P., McAlister, H. A., Raghavan, D., et al. 2011, ApJ, 728, 111
Öpik, E. 1932, PTarO, 27, 5
Pan, X. P., Shao, M., Colavita, M. M., et al. 1990, ApJ, 356, 641
Pourbaix, D. 2000, A&AS, 145, 215
Raghavan, D., McAlister, H. A., Torres, G., et al. 2009, ApJ, 690, 394
Ribas, I., Solano, E., Masana, E., & Giménez, A. 2003, A&A, 411, L501
Sturmann, J., ten Brummelaar, T. A., Sturmann, L., & McAlister, H. A. 2010, Proc. SPIE, 7734, 119
Tallon-Bosc, I., Tallon, M., Thiébaut, E., et al. 2008, Proc. SPIE, 7013, 44
ten Brummelaar, T. A., McAlister, H. A., Ridgway, S. T., et al. 2005, ApJ, 628, 453
ten Brummelaar, T. A., O'Brien, D. P., Mason, B. D., et al. 2011, AJ, 142, 21
ten Brummelaar, T. A., Sturmann, J., McAlister, H. A., et al. 2012, Proc. SPIE, 8445, 123
ten Brummelaar, T. A., Sturmann, J., Ridgway, S. T., et al. 2013, JAI, 2, 1340004
Tokovinin, A. A. 1992, in ASP Conf Ser. 32, Complementary Approaches to Double and Multiple Star Research, ed. H. A. McAlister & W. I. Hartkopf (IAU Colloquium 135; San Francisco, CA: ASP), 573
Tokovinin, A. A. 1993, AstL, 19, 73
Tokovinin, A. A., Griffin, R. F., Balega, Y. Y., Pluzhnik, E. A., & Udry, S. 2000, AstL, 26, 116
van Leeuwen, F. 2007, A&A, 474, 653
Vickers, C. R., & Scarfe, C. D. 1976, PASP, 88, 944
Wittenmyer, R. A., Endl, M., Cochran, W. D., Levison, H. F., & Henry, G. W. 2009, ApJS, 182, 97

[7] LITpro software available at http://www.jmmc.fr/litpro